Spectroscopic studies on glassy Ni(II) and Co(II) polyphosphate coacervates

ARTICLE *in* MATERIALS CHEMISTRY AND PHYSICS · NOVEMBER 2010

Impact Factor: 2.26 · DOI: 10.1016/j.matchemphys.2010.07.008

Materials Chemistry and Physics 124 (2010) 547–551

Contents lists available at ScienceDirect

Materials Chemistry and Physics

journal homepage: www.elsevier.com/locate/matchemphys

Spectroscopic studies on glassy Ni(II) and Co(II) polyphosphate coacervates

Maurício A.P. Silva[a,*], Douglas F. Franco[a], Adilson R. Brandão[a], Hernane Barud[b], Francisco A. Dias Filho[c], Sidney J.L. Ribeiro[b], Younès Messaddeq[b], Luiz F.C. de Oliveira[a]

[a] Núcleo de Espectroscopia e Estrutura Molecular, Departamento de Química, Universidade Federal de Juiz de Fora, Campus Universitário Martelos, 36036-900 Juiz de Fora, MG, Brazil
[b] Instituto de Química, Universidade Estadual Paulista, C.P. 355, 14801-970 Araraquara, SP, Brazil
[c] Departamento de Química Orgânica e Inorgânica, Centro de Ciências, Universidade Federal do Ceará, Campus do Pici, C.P. 12200, 60455-760 Fortaleza, CE, Brazil

ARTICLE INFO

Article history:
Received 22 September 2009
Received in revised form
25 November 2009
Accepted 8 July 2010

Keywords:
Amorphous materials
Glasses
Raman spectroscopy and scattering
Optical properties

ABSTRACT

Transparent amorphous bulk materials have been prepared through the coacervation process of sodium polyphosphate and Ni^{2+} and Co^{2+} chloride solutions. Structural and spectroscopic properties were analyzed by X-ray diffraction, thermogravimetric analysis, UV–vis, infrared and Raman spectroscopic techniques. Different optical properties and water absorption tendencies were observed for the polyphosphate coacervates. The symmetric $P–O_b$ and $P–O_t$ stretching modes on the Raman spectra for the coacervates and the sodium polyphosphate revealed the coordination processes of the polyphosphate chains to the metal ions, including the effects of the water coordination outside the polyphosphate cages, connecting the adjacent chains. Based on data collected from the electronic spectra, these materials can present important technological applicability. Being transparent materials, these glasses can be used as absorption filters with pass-band between 600 and 500 nm for the Ni coacervate, and above 600 nm for the Co coacervate.

1. Introduction

Polyphosphate coacervates are amorphous substances obtained through the destabilization of polyphosphate colloidal solutions, when a phase separation occurs, forming a water-insoluble denser phase. The coacervate, i.e., denser phase composed mainly by the longer polyphosphate chains and metal ions, becomes a vitreous solid when the water excess is eliminated (e.g. in a silica-gel dessicator). The "coacervate route" is proposed as a very important strategy to the production of polyphosphate glasses at room temperature. In fact, this simple synthesis method consists in the mixture of high concentration solutions of sodium polyphosphate $(NaPO_3)_n$, commercially known as Graham's salt) and electrolytes, such as calcium and magnesium chlorides. The phase separation appears instantly, and the separation from the supernatant (consisted of shorter polyphosphate chains and ions such as Cl^- and Na^+) is easily performed. This is a very well known phenomenon and has been investigated in the last three decades. For instance, Umegaki and Kanazawa [1] studied the temperature dependence of the viscoelastic behavior of magnesium coacervates. Kanazawa et al. [2] studied the solubility of coacervates of magnesium, calcium and aluminium in acid solutions. They used electrical conductivity, viscosity and paper chromatography measurements, and concluded that the coacervates dissolve into acid solvents without cleavage of the phosphate chains. Umegaki and Kanazawa [3] studied the viscosities of magnesium and calcium coacervates at various temperatures and were able to calculate their activation energy of flow to be about 7 kcal mol^{-1} and 15 kcal mol^{-1}, respectively. Umegaki et al. [4] determined the different crystalline phases that form under the thermal decomposition of magnesium coacervates, by means of DTA, TGA and high temperature X-ray diffraction techniques. Umegaki and Kanazawa [5] studied the degradation of magnesium and calcium coacervates, using viscosity and chromatographic analysis. Palavit et al. [6] reported the preparation of zinc-sodium phosphate glass precursors by coacervation. Gomez et al. [7] used the "coacervate route" to prepare sodium-calcium polyphosphate glasses, by melting the coacervates at 1000 °C for 1 h, to eliminate free water, and studied the dehydroxylation mechanisms of the glasses in relation to temperature and pressure. The same authors [8] used the coacervation process for the preparation of polyphosphate glasses and characterized them using Controlled-transformation Rate Thermal Analysis (CRTA). Willot et al. [9] studied the physical properties of zinc-sodium polyphosphate glasses, using the coacervate route. Dias Filho et al. [10] used Eu^{3+} luminescence properties to probe the coacervation process. They proposed the occurrence of two main families of sites for the metal ions in the aqueous polyphosphate colloidal systems: cage-like sites provided by the polyphosphate chain and a family of sites which arises following saturation of the cagelike sites. In their interpretation, the coacervation process starts by the occupation of this

* Corresponding author. Tel.: +55 32 2102 3310.
E-mail address: mauricio.silva@ufjf.edu.br (M.A.P. Silva).

0254-0584/$ – see front matter © 2010 Elsevier B.V. All rights reserved.
doi:10.1016/j.matchemphys.2010.07.008

second family of sites, which leads to supramolecular interactions between polyphosphate chains and the consequent destabilization of the colloidal system.

Recently we have studied the structural properties of a new composition of polyphosphate coacervates, containing the transition metal ions Ni^{2+} and Co^{2+} [11]. The coacervation process, as proposed in Ref. [10], was analyzed by X-ray Absorption Spectroscopy (through EXAFS analysis) and FT-Raman Spectroscopy, and the results corroborate the cited proposition.

In this work we explore some structural and spectroscopic properties of the polyphosphate coacervates containing Ni^{2+} and Co^{2+} ions, by means of X-ray diffraction, thermogravimetric analysis, UV–vis, infrared and Raman spectroscopies.

2. Experimental

To a 4 mol L^{-1} $(NaPO_3)_n$ solution kept under constant stirring an equal volume of 1 mol L^{-1} MCl_2 (M = Ni or Co) solution was added. Following the method proposed by Umegaki et al. [4] methyl alcohol was added (10% in volume) to the solution, in order to obtain the liquid–liquid phase separation, being the coacervate collected as the denser phase. The viscous green-coloured Ni coacervate and purple-coloured Co coacervate were maintained for two days in a vacuum silica-gel dessicator, and the transparent glassy materials were submitted to structural, thermal and spectroscopic studies.

Powder X-ray diffraction measurements were carried out with a D5000 Siemens diffractometer using Cu Kα radiation. The 2θ investigation region was in the range of 4–70° with a step pass of 0.05° and a step time of 1 s.

Thermogravimetric (TG) measurements were carried out in a Thermal Analyst 3100 calorimeter from TA Instruments, under N_2 atmosphere. Powdered samples were set in sealed aluminum pans and heated at a constant rate $q = 10\,K\,min^{-1}$.

A Shimadzu UV/vis spectrophotometer PC1601 was used to record the UV/vis aqueous solutions of the metal ions, as well the spectra of the solids. The reflectance spectra of all samples were obtained from an Ocean Optics spectrometer USB2000 fiber optic instrument, in the range 350–1100 nm.

Infrared spectra of the samples in KBr pellets were obtained in a Bomem FT instrument model MB102, from 4000 to 400 cm^{-1}, using 4 cm^{-1} as spectral resolution and a good signal/noise ratio with 128 scans.

FT-Raman spectra were measured using a Bruker RFS 100 instrument equipped with Nd^{3+}/YAG laser operating at 1064 nm in the near infrared, and a CCD detector cooled with liquid N_2; the spectral resolution was kept at 4 cm^{-1}, and good signal/noise ratio were achieved by 500 spectra accumulations, with 50 mW of laser power at the sample.

3. Results

X-ray diffraction patterns are shown in Fig. 1, and indicate that the coacervates are essentially amorphous. Two narrow peaks appearing at 31.5°, 45.5° and 56.3° can be assigned to excess NaCl that could be removed by repetitive washing with distilled water.

Fig. 2 shows the thermogravimetric curves for the Ni^{2+} and Co^{2+} coacervates, where important water release processes are observed, but also reflects the hygroscopicity tendency of these samples, as discussed below.

In Fig. 3, UV–vis absorption spectra are shown for the coacervate samples. As a comparison, this analysis was also performed for Ni^{2+} and Co^{2+} aqueous solutions. Fig. 4 shows the UV–vis diffuse reflectance spectra of the glassy samples.

Fig. 5 shows infrared absorption spectra obtained for the Ni^{2+} and Co^{2+} coacervates, and also for the $(NaPO_3)_n$. Table 1 shows the vibrational frequencies assigned to characteristic vibrational modes of the phosphate groups [12–20].

The Raman spectra obtained for the Ni^{2+} and Co^{2+} coacervates and the $(NaPO_3)_n$ are depicted in Fig. 6.

4. Discussion

The thermogravimetric curves in Fig. 2 show that for the Co^{2+} coacervate about 10% of mass is lost as water release at 100 °C, while for the Ni^{2+} coacervate only 2.5% of mass was lost at that temperature. In fact in previous EXAFS studies [11], some of us have shown the higher disorder in the first coordination shell of the cobalt

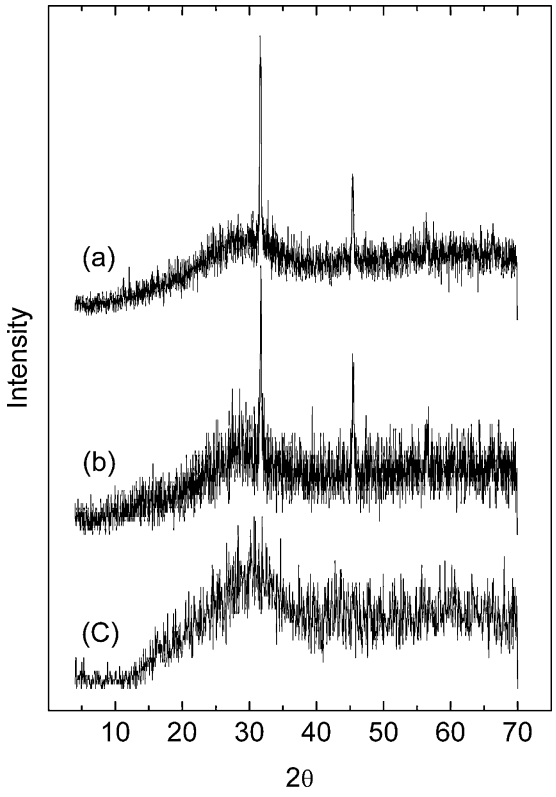

Fig. 1. X-ray diffraction (XRD) for the samples: (a) cobalt coacervate; (b) nickel coacervate; (c) $(NaPO_3)_n$.

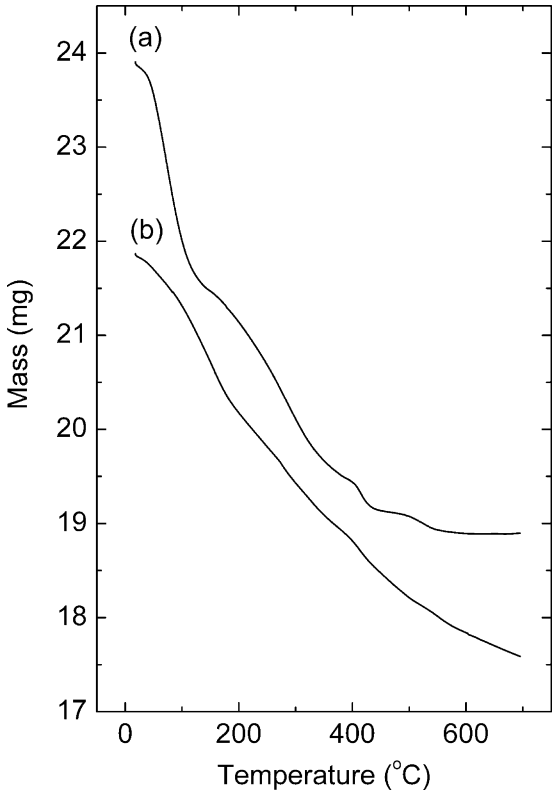

Fig. 2. Thermal gravimetric (TG) curve for: (a) cobalt coacervate and (b) nickel coacervate.

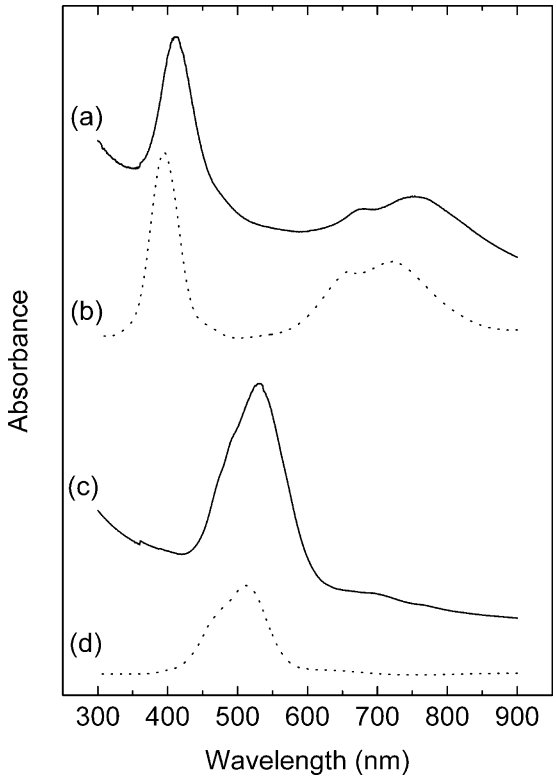

Fig. 3. UV/vis spectra for the samples: (a) nickel coacervate; (b) Ni^{2+} aqueous solution; (c) cobalt coacervate; (d) Co^{2+} aqueous solution.

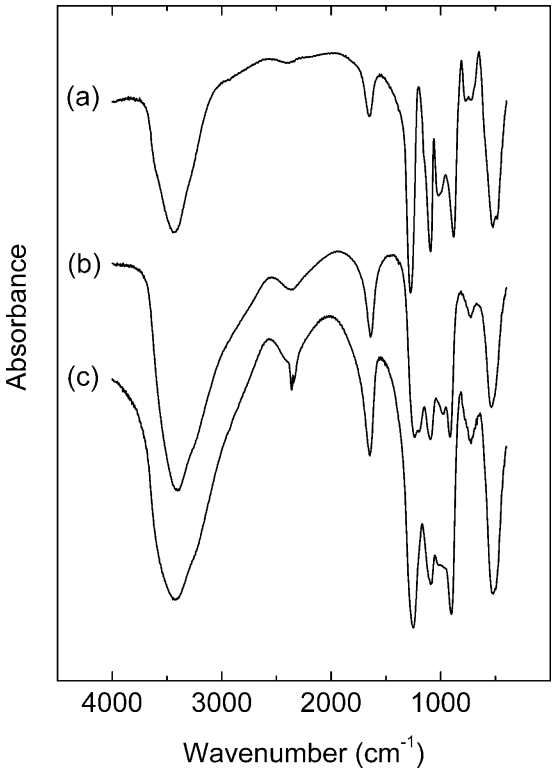

Fig. 5. Infrared vibrational spectra for: (a) $(NaPO_3)_n$; (b) nickel coacervate; (c) cobalt coacervate.

ions, reflecting the higher hygroscopicity tendency revealed by the Co coacervates. The strongly endothermic water release hidden the glass-transition range in the Differential Scanning Calorimetry analysis (DSC) not shown here. The thermogravimetric analysis indicated that a considerable quantity of water remains in the coacervate structure, even after complete drying in a vacuum silica-gel dessicator. This result is consistent with the infrared spectroscopy results, as discussed below.

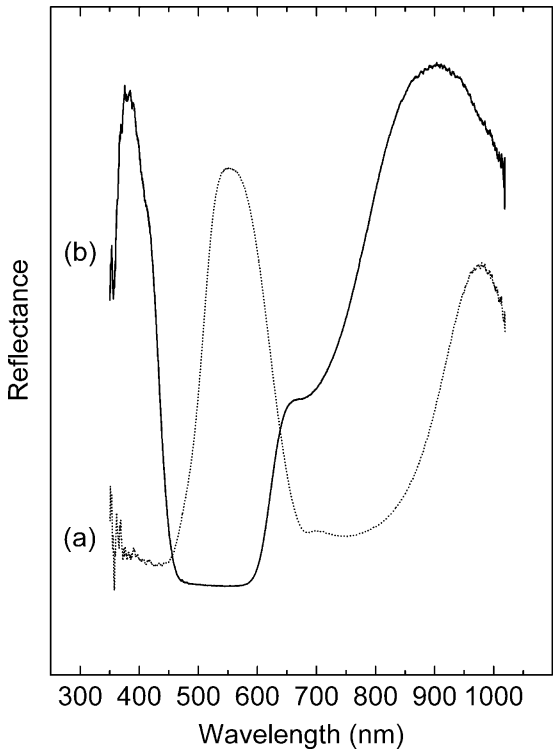

Fig. 4. UV/vis diffuse reflectance for the coacervate samples: (a) nickel coacervate and (b) cobalt coacervate.

Clear similarities between the UV–vis absorption spectra of the coacervates and the respective hydrated ions, are observed in Fig. 3. A 20 nm red-shift is observed for the coacervates. Absorption bands centered at 415 and 395 nm are observed for the Ni^{2+} coacervate and aqueous solution, respectively. Absorption bands at 533.5 and 512.5 nm are observed for the Co^{2+} coacervate and aqueous solution, respectively. The red-shift observed for coacervates can be attributed to the additional interaction of the metal ions with the coordinating phosphate units of the polyphosphate chain. In fact from previous studies some of us have concluded for cagelike sites available for metal ions [11].

As expected, wavelength regions of maximum reflectivity are present where the compounds present the minimum electronic absorption and this was observed in the diffuse reflectance spectra shown in Fig. 4. Based on the data collected from the electronic

Table 1
Characteristic vibrational wavenumbers for different phosphate species. IR: infrared active bands; R: Raman active bands.

Structural group	Wavenumber range (cm^{-1})	Reference
δ_s (PO_4^{3-})	~560 (IR)	[12]
ν_s (P–O_b)	690 (R)	[22,23]
ν_{as} (P–O–P) (linear)	700 (IR)	[13]
ν_s (P–O–P)	725 and 780 (IR)	[14]
ν_{as} (P–O–P) (linear)	900 (IR)	[13]
(PO_3) (terminal)	~1030 (IR)	[15]
$(P–O)^-$ (terminal)	~1100–1000 (IR)	[16]
ν_s (P–O_t)	1160 (R)	[22,23]
ν_s $(PO_2)^-$ (chain species)	~1160 (IR)	[17,18]
ν_{as} $(PO_2)^-$ (chain species)	~1270 (IR)	[19]
P–O–H	~2700 (IR)	[20]

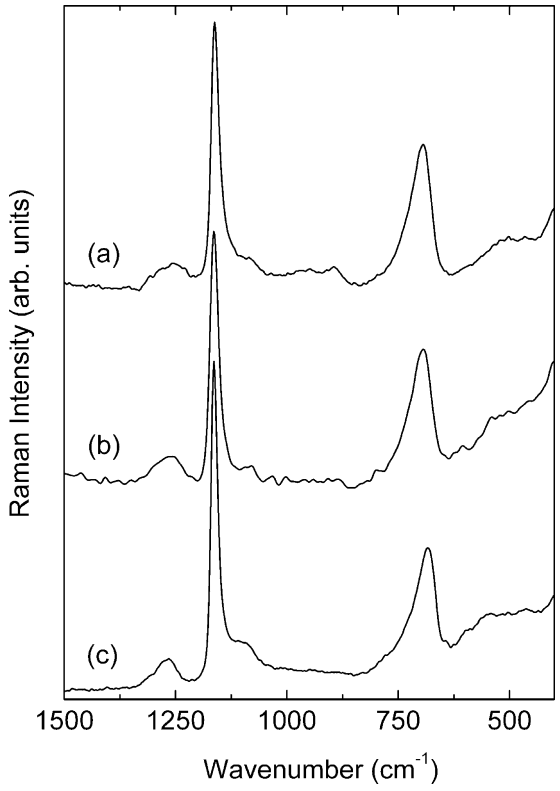

Fig. 6. Raman scattering spectra for: (a) cobalt coacervate; (b) nickel coacervate; (c) $(NaPO_3)_n$.

spectra of Figs. 3 and 4, these materials can present important technological applicability. Being transparent materials, these glasses can be used as absorption filters with pass-band between 600 and 500 nm for the Ni coacervate, and above 600 nm for the Co coacervate.

Fig. 5 reveals that the Ni^{2+} and Co^{2+} coacervates present similar vibrational behavior to the one obtained for the polyphosphate. The bands at 1272 and 1154 cm^{-1} can be assigned, respectively, to the asymmetric and symmetric stretching of the units (PO_2) containing non-bonding oxygen atoms in the middle of the chain. The band at 1090 cm^{-1} can be assigned to the stretching of the terminal groups $P–O^-$ and the one at 1028 to the terminal PO_3 groups. The band appearing at 882 cm^{-1} in the spectra of Fig. 5 is strongly influenced by the condensation of the phosphate units that build the chains. It is attributed to the asymmetric stretching modes of the P–O–P groups in the middle of the chain. Originally occurring at 900 cm^{-1}, this band is shifted to lower wavenumbers due to the longer chains in the glassy $(NaPO_3)_n$ and in the coacervates. The symmetric stretching of the P–O–P groups are reflected by the bands in the 722 and 783 cm^{-1} range, and the band at ca. 520 cm^{-1} is attributed to the P–O deformation modes in the PO_4^{-3} groups. Moreover, the vibrational spectra of the coacervates and $(NaPO_3)_n$ present two bands around 1650 and 3450 cm^{-1}, attributed to the deformation and stretching modes of adsorbed water molecules. The infrared spectra presented in Fig. 5 show that the metal coacervates have the same vibrational behavior as the glassy $(NaPO_3)_n$ and, considering the bands related to the bridging structures in the chains (1272, 1154, 882, 722 and 783 cm^{-1}), we conclude that the polyphosphate chains in the coacervates do not bear any kind of break of the bonds caused by the presence of the metallic ions [21].

The main bands, in the regions of 690 and 1160 cm^{-1} of the Raman spectra of the Ni^{2+} and Co^{2+} coacervates and the $(NaPO_3)_n$, as shown in Fig. 6, can be assigned to $P–O_b$ (bridged) and $P–O_t$ (terminal) symmetric stretching modes, respectively, very characteristic of the vibrational spectra of polyphosphate materials [22,23]. These bands are centered at 694 and 1164 cm^{-1} for the Ni^{2+} coacervate, at 694 and 1162 cm^{-1} for the Co^{2+} coacervate and at 684 and 1164 cm^{-1} for the $(NaPO_3)_n$. Despite the small differences in wavenumber, the behavior of these vibrational modes indicates the changes in the vibrational behavior of the PO_4 groups, induced by the presence of the transition metal. The shift to higher wavenumber of the symmetric $P–O_b$ stretching mode can be explained by means of the force constant of the $P–O_b$ bonds. An increasing in the $P–O_b$ bond strength is caused by the presence of the transition metal ions bonded to the terminal oxygen atoms, O_t–M bonds.

In the first stages of the coacervation process, when a small quantity of transition metal is added to the sodium polyphosphate solution, an accentuated wavenumber decrease of the $P–O_t$ symmetric stretching mode is observed, compared to $(NaPO_3)_n$ (1158 cm^{-1} for the coacervate with molar ratio P/Co = 10, and 1164 cm^{-1} for the initial Graham's salt) [11]. As discussed in Ref. [11], at high P/M^{2+} concentration ratio the transition metal ions are predominantly situated inside cagelike sites, formed by the long polyphosphate chains. When the ion concentration increases, e.g. from P/M^{2+} = 10 to 4, the sites inside the polyphosphate cages are saturated and the coacervation process begins due to metal ions induced supramolecular interactions. Under such conditions the metal ions are more exposed to interactions with water molecules, leading to a decrease of the electronic density of the O_t–M bonds and, consequently, an increase of the $P–O_t$ and $P–O_b$ bond strengths. This fact is reflected in the shift to higher wavenumbers of the $P–O_t$ symmetric stretching modes of the coacervates with P/M^{2+} = 10–4 (from 1158 to 1162 cm^{-1}, respectively) [11]. So, in the present case (P/M^{2+} = 4), similar wavenumber values for the $P–O_t$ symmetric stretching modes between the Ni coacervate (1164 cm^{-1}), Co coacervate (1162 cm^{-1}) and the sodium polyphosphate (1164 cm^{-1}) are observed. Moreover, the relatively large wavenumber red-shift for the symmetric $P–O_b$ stretching mode of the coacervates (694 cm^{-1}), compared to the $(NaPO_3)_n$ (684 cm^{-1}), can be related to the increase of the $P–O_b$ bond strengths when metal concentration increases. The presence of more O_t–M bonds in the coacervate causes a decrease in the electronic density around the $P–O_t$ bonds, leading to an increase of $P–O_b$ bond strength.

5. Conclusions

Polyphosphate coacervates were prepared with the transition metal ions Ni^{2+} and Co^{2+}. The glassy samples presented amorphous X-ray diffraction pattern. The higher tendency of water absorption was confirmed for the Co coacervate, as predicted in our previous work [11]. The metallic ions in the coacervates and in solution have similar electronic spectra, indicating that the first coordination shell of the metal is composed of the six water molecules of the aquo ion $[M(H_2O)_6]^{2+}$. This is also in agreement with our previous EXAFS studies [11], although the interaction between the metal ions and the oxygen atoms from the polyphosphate species was also proposed. The infrared spectra reveal the similarities on the vibrational behavior between the coacervates and the sodium polyphosphate, indicating that there is no noticeable break of the bonds in the polyphosphate chains. The symmetric $P–O_b$ and $P–O_t$ stretching modes on the Raman spectra for the coacervates and the sodium polyphosphate revealed the coordination processes of the metallic ion to the polyphosphate chains, including the effects of the water coordination in the metallic ions outside the polyphosphate cages, connecting the adjacent chains.

Acknowledgments

The financial support of FAPEMIG, FAPESP, CNPq and CAPES/PROINFRA (Brazilian agencies) is gratefully acknowledged.

References

[1] T. Umegaki, T. Kanazawa, Bull. Chem. Soc. Jpn. 46 (1973) 3587.
[2] T. Kanazawa, T. Umegaki, Y. Kitamija, T. Ogawa, Bull. Chem. Soc. Jpn. 47 (1974) 1419.
[3] T. Umegaki, T. Kanazawa, Bull. Chem. Soc. Jpn. 48 (1975) 1452.
[4] T. Umegaki, Y. Nakayama, T. Kanazawa, Bull. Chem. Soc. Jpn. 49 (1976) 2105.
[5] T. Umegaki, T. Kanazawa, Bull. Chem. Soc. Jpn. 52 (1979) 2124.
[6] G. Palavit, L. Montagne, R. Delaval, J. Non-Cryst. Solids 189 (1995) 277.
[7] F. Gomez, P. Vast, Ph. Llewellyn, F. Rouquerol, J. Non-Cryst. Solids 222 (1997) 415.
[8] F. Gomez, P. Vast, Ph. Llewellyn, F. Rouquerol, J. Therm. Anal. 49 (1997) 1171.
[9] G. Willot, F. Gomez, P. Vast, V. Andries, M. Martines, Y. Messaddeq, M. Poulain, C. R. Chim. 5 (2002) 899.
[10] F.A. Dias Filho, L.D. Carlos, Y. Messaddeq, S.J.L. Ribeiro, Langmuir 21 (2005) 1776.
[11] M.A.P. Silva, D.F. Franco, L.F.C. de Oliveira, J. Phys. Chem. A 112 (2008) 5385.
[12] K. Nakamoto, Infrared and Raman Spectra of Inorganic and Coordination Compounds, Wiley-Interscience, New York, 1986.
[13] C. Dayanand, G. Bhikshamaiah, T.V. Jaya, M. Salagram, A.S.R.K. Murthy, J. Mater. Sci. 31 (1996) 1945.
[14] S. Honkanen, S.I. Najafi, P. Poyhonen, G. Orcel, W.J. Wang, J. Chrostowski, Electron. Lett. 27 (1991) 2167.
[15] D.E. Corbridge, J. Appl. Chem. 6 (1956) 456.
[16] R. Bartholomew, J. Non-Cryst. Solids 7 (1972) 221.
[17] R.M. Supkowski, W.D. Horrocks Jr., Inorg. Chem. 38 (1999) 5616.
[18] D.L. Veasey, D.S. Funk, P.M. Peters, N.A. Sanford, G.E. Obarski, N. Fontaine, M. Young, A.P. Peskin, W.C. Liu, S.N.H. Walter, J.S. Hayden, J. Non-Cryst. Solids 263 (2000) 369.
[19] L.C. Barbosa, N. Aranha, O.L. Alves, R. Srivastava, Electron. Lett. 20 (1996) 1919.
[20] R.M. Almeida, J.D. Mackenzie, J. Non-Cryst. Solids 40 (1980) 535.
[21] F.A. Dias Filho, PhD Thesis, Instituto de Química de Araraquara, UNESP, Brazil, 2003.
[22] D.I. Novita, P. Boolchand, Phys. Rev. B 76 (2007) 184205.
[23] M. Weil, M. Puchberger, J.S. auf der Günne, J. Weber, Chem. Mater. 19 (2007) 5067.